molecular pharmaceutics

Article

Cite This: Mol. Pharmaceutics 2018, 15, 3664−3671

GE11-Directed Functional Polymersomal Doxorubicin as an Advanced Alternative to Clinical Liposomal Formulation for Ovarian Cancer Treatment

Yan Zou,[†,‡] Yifeng Xia,[†] Fenghua Meng,[*,†] Jian Zhang,[†] and Zhiyuan Zhong[*,†]

[†]Biomedical Polymers Laboratory, and Jiangsu Key Laboratory of Advanced Functional Polymer Design and Application, College of Chemistry, Chemical Engineering and Materials Science, Soochow University, Suzhou 215123, P. R. China

[‡]International Joint Centre for Biomedical Innovation, School of Life Sciences, Henan University, Jin Ming Avenue, Kaifeng, Henan 475004, China

Supporting Information

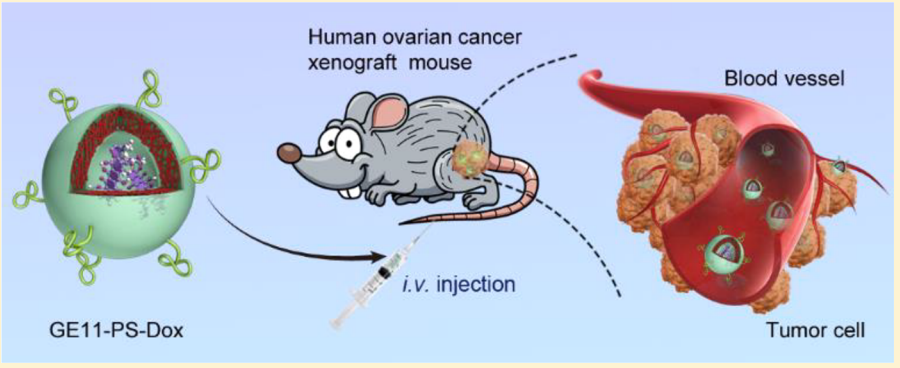

ABSTRACT: Ovarian cancer as a recurrent disease is often refractory to treatment including pegylated liposomal doxorubicin hydrochloride (Lipo-Dox). Here, GE11 peptide-modified reversibly cross-linked polymersomal doxorubicin (GE11-PS-Dox) was investigated as an advanced treatment for SKOV3 human ovarian tumors, which overexpress epidermal growth factor receptor (EGFR). The *in vitro* experiments using SKOV3 cancer cells demonstrated that GE11-PS-Dox induced obviously higher cellular uptake, Dox delivery to the nuclei, and antitumor activity than the nontargeted PS-Dox and Lipo-Dox controls. *In vivo* biodistribution experiments displayed 2.5-fold higher tumor accumulation for GE11-PS-Dox as compared to Lipo-Dox. Notably, GE11-PS-Dox could effectively suppress the progression of SKOV3 tumors and cause little adverse effects at 12 mg of Dox equiv/kg, leading to a remarkably increased survival rate of 100% over 78 days. In contrast, continued tumor growth and body weight loss were discerned for Lipo-Dox treated mice at 6 mg of Dox equiv/kg. Moreover, a single dose of GE11-PS-Dox at 60 mg of Dox equiv/kg showed also effective treatment and low toxicity toward SKOV3-tumor bearing mice. GE11-directed reversibly cross-linked polymersomal doxorubicin has emerged as an advanced alternative to Lipo-Dox for treatment of EGFR-overexpressing ovarian cancers.

KEYWORDS: *epidermal growth factor receptor, polymersomes, reduction-sensitive, targeted delivery, ovarian cancer*

INTRODUCTION

Ovarian cancer as a recurrent disease is often refractory to treatment and becomes worldwide the most lethal gynecological malignancy.[1−5] Various nanomedicines have recently been proposed and explored for ovarian cancer therapy.[6−11] Notably, pegylated liposomal doxorubicin hydrochloride (Doxil, refers to as Lipo-Dox) is currently used for treating ovarian cancer patients.[12−14] Lipo-Dox, while capable of reducing the cardiotoxicity of doxorubicin (Dox), affords new adverse effects like hand−foot syndrome and stomatitis.[15,16] To achieve better therapeutic outcomes, liposomes have been functionalized with different ligands such as peptide, folate, antibody, and transferrin.[17−21] For example, Di et al. reported that epidermal growth factor (EGF)-modified liposomes loaded with cisplatin−alginate conjugate showed targeted treatment of EGFR-positive SKOV3 ovarian tumor-bearing mice.[22] GE11 peptide (YHWYGYTPQNVI) has shown a high affinity to EGFR overexpressing cancer cells including ovarian, hepatoma, colon cancer, and lung cancer cells.[23−26] Xu et al. reported that GE11-targeted liposomal doxorubicin displayed fast tumor accumulation and improved treatment of SMMC-7 human hepatoma as compared to nontargeted liposomal doxorubicin.[27]

Special Issue: New Directions for Drug Delivery in Cancer Therapy

Received: January 9, 2018
Revised: March 20, 2018
Accepted: March 23, 2018
Published: March 23, 2018

DOI: 10.1021/acs.molpharmaceut.8b00024
Mol. Pharmaceutics 2018, 15, 3664−3671

Notably, ligand-decorated liposomal formulations typically show a moderate tumor-targetability, partially due to their reduced *in vivo* stability.

Polymersomes are an attractive alternative to liposomes.[28,29] Notably, polymersomes are generally more stable[30−33] and easy to be functionalized with varying targeting ligands and stimuli-sensitivity.[34−39] Interestingly, disulfide-cross-linked polymersomes were shown to possess not only further improved stability but also fast intracellular drug release, leading to significantly enhanced treatment efficacy in various tumor models such as B16F10 melanoma and H460 and A549 human lung cancers.[40−43] We recently found that GE11-modified reversibly cross-linked polymersomal doxorubicin (GE11-PS-Dox) based on poly(ethylene glycol)-poly(trimethylene carbonate-*co*-dithiolane trimethylene carbonate) (PEG-P(TMC-DTC)) block polymer demonstrated a high toleration in mice and efficacious treatment of orthotopic SMMC 7721 liver tumor-bearing mice.[44]

Inspired by its EGFR targeting ability, we hereby investigated GE11-PS-Dox as an advanced treatment option to clinically used Lipo-Dox for SKOV3 human ovarian cancer (Scheme 1).

Scheme 1. Illustration of GE11-Directed Reversibly Crosslinked Polymersomal Doxorubicin (GE11-PS-Dox) for Targeted Treatment of EGFR-Overexpressing SKOV3 Human Ovarian Cancers *in Vivo*

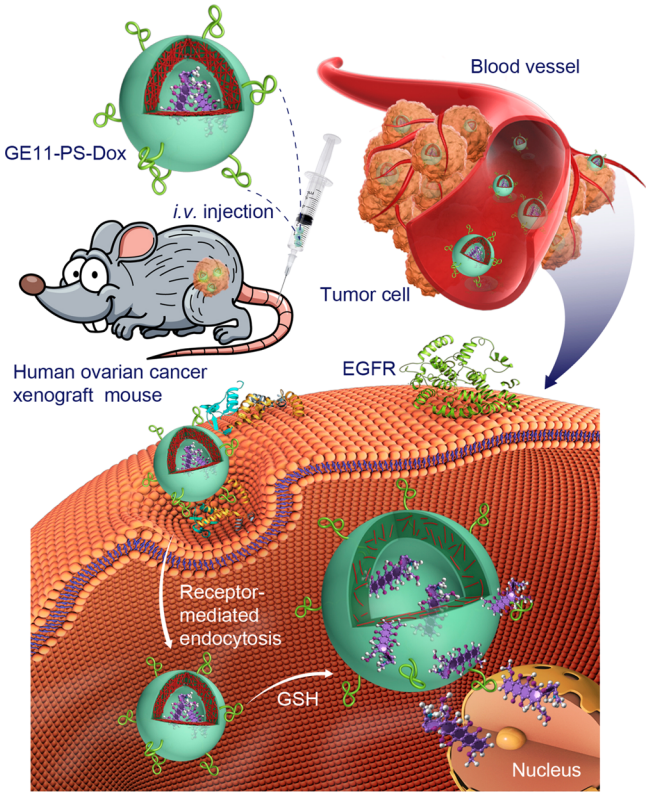

In contrast to EGF, short GE11 peptide does not activate EGFR.[45] GE11 can also combine with other ligands like hyaluronic acid to achieve synergistic targeting ability to ovarian cancers.[46] Interestingly, our results demonstrated that GE11-PS-Dox, given either in multiple or single dosage scheme, exhibits significantly enhanced therapeutic efficacy and lower adverse effects as compared to Lipo-Dox in treating SKOV3 tumor-bearing mice. This GE11-directed functional polymersomal doxorubicin has a great potential as an advanced alternative to Lipo-Dox for treatment of EGFR-overexpressing ovarian cancers.

EXPERIMENTAL SECTION

Preparation of GE11-PS-Dox and PS-Dox. GE11-PS-Dox were prepared from co-self-assembly of PEG-P(TMC-DTC) and YHWYGYTPQNVI-functionalized PEG-P(TMC-DTC) (GE11-PEG-P(TMC-DTC)) in aqueous solution followed by loading doxorubicin hydrochloride (Dox·HCl) via a pH-gradient method, as reported previously.[44] Briefly, to 2.7 mL of citric acid buffer (10 mM, pH 4.0) was added 300 μL of *N*,*N*-dimethylformamide (DMF) solution of PEG-P(TMC-DTC) and GE11-PEG-P(TMC-DTC) (10.0 mg/mL) at a molar ratio of 80/20. After 4 h, the pH of polymersome dispersion was adjusted to 7.8, Dox·HCl aqueous solution (5 mg/mL) was added at a theoretical drug loading content (DLC) of 16.7 wt %, and the dispersion following 5 h stirring at 37 °C was extensively dialyzed against PB (10 mM, pH 7.4). Dynamic light scattering (DLS) measurements showed that thus obtained GE11-PS-Dox had a hydrodynamic size of 92 nm and polydispersity index (PDI) of 0.12. Fluorometry measurement revealed a DLC of 11.6 wt %. In a similar way, PS-Dox was prepared from PEG-P(TMC-DTC) alone with a size of 89 nm (PDI 0.11) and DLC of 11.4 wt %.

Flow Cytometry Analyses and Confocal Microscopy Measurements. SKOV3 cells in a 6-well plate (1×10^6 cells/well) following 4 h incubation with GE11-PS-DOX or pegylated liposomal doxorubicin (Lipo-Dox, LIBOD, Shanghai Fudan-Zhangjiang Bio-Pharmaceutical Co., Ltd.) in 500 μL of PBS (10 μg of Dox·HCl equiv/mL) at 37 °C were digested by using 0.25% (w/v) trypsin and 0.03% (w/v) EDTA. After centrifugation (1000 × *g*, 3 min) the suspensions were washed (PBS, ×2) and resuspended in 500 μL of PBS for immediate measurements of fluorescence histograms with a BD FACS Calibur flow cytometer (Becton Dickinson, USA) and analysis using Cell Quest software based on 10,000 gated events. The gate was arbitrarily set for the detection of fluorescence at 488 nm.

SKOV3 cells were cultured on microscope coverslips in 24-well plates (1×10^5 cells/well). GE11-PS-Dox or Lipo-Dox in 50 μL of PBS (10 μg of Dox·HCl equiv/mL) were added and incubated for 4 h at 37 °C, followed by replacing the medium with a fresh one. After further culturing for 8 h, the cells on microscope coverslips were washed (PBS, ×3) and fixed with 4% paraformaldehyde solution for 15 min. Fluorescein isothiocyanate labeled phalloidin (phalloidin-FITC) was added to stain the cytoskeleton for 1 h. 4′,6-Diamidino-2-phenylindole (DAPI) was added to stain the nuclei for 10 min. Each step was followed by washing (PBS, ×3). A confocal microscope (TCS SP5, Leica) was used to obtain the fluorescence images.

Animal Models. All animal experiments were approved by the Animal Care and Use Committee of Soochow University and all protocols conformed to the Guide for the Care and Use of Laboratory Animals. The subcutaneous SKOV3 tumor xenograft model was established by inoculating SKOV3 cells (5×10^6) in 50 μL of PBS into the right hind flank of female Balb/c nude mice (18−20 g) for 2 weeks. The tumors of 200 mm^3 were excised, cut into pieces, and transplanted into the left hind flank of mice. The mice with tumor size of ca. 100 and 200−300 mm^3 were used for *in vivo* treatment and biodistribution studies, respectively.

DOI: 10.1021/acs.molpharmaceut.8b00024
Mol. Pharmaceutics 2018, 15, 3664−3671

***In Vivo* Near-Infrared Imaging.** To monitor their biodistribution *in vivo* by fluorescence imaging, GE11-PS and PS were loaded with 5 wt % 1,1′-dioctadecyltetramethyl indotricarbocyanine iodide (DiR, 98%, AAT Bioquest Inc.) as described previously with slight modifications.[47] Briefly, 95 μL of DMF solution (5 mg/mL) of PEG-P(TMC-DTC) and GE11-PEG-P(TMC-DTC) (80/20, mol/mol) was mixed with 5 μL of dimethyl sulfoxide (DMSO) solution of DiR (5 mg/mL) and injected into 900 μL of PB (10 mM, pH 7.4). The dispersion was dialyzed for 12 h against PB buffer, yielding DiR-loaded GE11-PS (GE11-PS-DiR) with a hydrodynamic size of ca. 90 nm (PDI 0.12) and a DiR loading content of ca. 4.0 wt %. DiR-loaded PS (PS-DiR) with a size of ca. 88 nm (PDI 0.11) and DiR loading content of ca. 4.1 wt % was prepared from PEG-P(TMC-DTC) alone. Thus, obtained GE11-PS-DiR and PS-DiR were intravenously injected into SKOV3 tumor-bearing mice via tail veins (n = 3). At predetermined time, the mice were anesthetized with isoflurane and scanned using an IVIS Lumina II near-infrared fluorescence imaging system (Ex. 747 nm, Em. 774 nm). During the image acquiring process, 3% isoflurane was continuously delivered via a nose cone system. The fluorescence images were acquired and analyzed using Lumina II software.

***Ex Vivo* Imaging and Biodistribution of GE11-PS-Dox.** A single dose of GE11-PS-Dox, PS-Dox, or Lipo-Dox in 200 μL of PBS was administrated intravenously into SKOV3 tumor-bearing mice (10 mg of Dox·HCl equiv/kg). After 8 h, the tumors and heart, liver, spleen, lung, and kidneys were excised, washed, dried with a paper towel, and weighed before acquiring their fluorescence images with IVIS Lumina II system. To quantify the Dox·HCl biodistribution, the tumor and organs were homogenized in 0.6 mL of 1% Triton X-100 at 18000 rpm for 10 min. Dox·HCl was extracted from tissue lysate by incubating with 900 μL of DMF solution containing 50 mM HCl and 20 mM DL-dithiothreitol (DTT) overnight. After centrifugation (14.8 krpm, 5 min), Dox·HCl concentration in the supernatant was quantified by fluorometry and expressed as injected dose per gram of tissue (%ID/g).

***In Vivo* Treatment of SKOV3 Ovarian Tumor.** SKOV3 tumor-bearing mice were weighed and randomly divided into five groups (n = 6). GE11-PS-Dox was intravenously injected at two different dosages, 6 or 12 mg of Dox·HCl equiv/kg, via tail vein on day 0, 3, 6, 9, and 12. Lipo-Dox and PS-Dox (dosage: 6 mg of Dox·HCl equiv/kg) as well as PBS were used as controls. The tumor size and body weight were measured every 3 days. The tumor volume was calculated according to $V = 0.5 \times L \times W^2$, wherein L and W are the tumor dimensions at the longest and widest points, respectively. The relative body weight was obtained by normalizing to the initial weight. On day 24, one mouse of each group was sacrificed, and the tumor, heart, liver, spleen, lung, and kidney were excised, washed, fixed with 4% paraformaldehyde solution, and embedded in paraffin. The organs were sliced (thickness: 4 mm) before staining with hematoxylin and eosin (H&E) for microscope observation (Leica). The Kaplan−Meier survival curve was determined within 78 days (n = 5). Mice in each cohort were considered dead either when the mice died during treatment or when the tumor volume reached 1000 mm^3.

We further studied the therapeutic efficacy of GE11-PS-Dox at a single dose of 60 mg of Dox·HCl equiv/kg (n = 5). A single dose of Lipo-Dox at 15 mg of Dox·HCl equiv/kg and PBS were used as controls. The body weight, tumor size, and survival rates were monitored as above.

Statistical Analyses. The difference between groups was assessed using one-way ANOVA with Tukey multiple comparisons tests using GraphPad Prism. Kaplan−Meier survival curves were analyzed by one-way ANOVA with a log-rank test for comparisons using GraphPad Prism 7. *p < 0.05 was considered significant; **p < 0.01 and ***p < 0.001 were highly significant.

RESULTS AND DISCUSSION

EGFR-Mediated Uptake and Intracellular Drug Release of GE11-PS-Dox in SKOV3 Human Ovarian Cancer Cells. Pegylated liposomal doxorubicin hydrochloride (Lipo-Dox) is a second-line therapy for ovarian cancers.[48] Lipo-Dox is also being actively investigated for clinical combination chemotherapy with carboplatin and gemcitabine.[49,50] Interestingly, we recently show that GE11-PS-Dox is superior to Lipo-Dox (PDI = 0.14), from both safety and efficacy points of view, in treating orthotopic SMMC 7721 liver tumor-bearing mice.[44] In this study, we were set to evaluate GE11-PS-Dox as a potential alternative to clinically used Lipo-Dox for *in vitro* and *in vivo* treatment of EGFR-overexpressing SKOV3 human ovarian cancers.

Both GE11-PS-Dox and nontargeted PS-Dox control were obtained with a Dox loading content of ca. 11.6 wt %, hydrodynamic size of ca. 90 nm. We first investigated the uptake and intracellular drug release of GE11-PS-Dox in SKOV3 cells. Notably, flow cytometric analyses showed significantly higher cellular uptake of GE11-PS-Dox than PS-Dox and Lipo-Dox (Figure 1A). The uptake of GE11-PS-Dox was 2.2- and 20-fold higher than PS-Dox and Lipo-Dox, respectively. The confocal microscopy displayed strong Dox fluorescence in SKOV3 nuclei after 4 h incubation with GE11-PS-Dox and another 8 h culture in fresh medium (Figure 1B), indicating Dox has been released from GE11-PS-Dox. Dox fluorescence was also observable in the nuclei of PS-Dox treated cells, though significantly weaker than that of GE11-PS-Dox. In contrast, negligible Dox fluorescence was discerned in the Lipo-Dox treated cells. These results reveal that GE11-PS-Dox mediates significantly more efficient uptake and faster drug release into the nuclei of SKOV3 cells than both PS-Dox and Lipo-Dox.

In accordance with the cellular uptake results, MTT assays showed that GE11-PS-Dox was much more potent against SKOV3 cancer cells than both PS-Dox and Lipo-Dox controls (Figure 1C). The half-maximal inhibitory concentration (IC_{50}) of GE11-PS-Dox was 8.7 Dox equiv/mL, which was about 1.9- and 3.7-fold lower than PS-Dox and Lipo-Dox, respectively. It is evident, therefore, that GE11-PS-Dox can actively target to SKOV3 cancer cells inducing far better anticancer effect *in vitro* than Lipo-Dox.

***In Vivo* Biodistribution in SKOV3 Tumor-Bearing Mice.** To monitor their biodistribution *in vivo* by fluorescence imaging, GE11-PS and PS were laden with a near-infrared (NIR) dye (5% DiR). *In vivo* fluorescence imaging revealed fast and strong accumulation of GE11-PS-DiR in the SKOV3 ovarian tumor (Figure 2A). The strongest tumor fluorescence was observed at 8 and 12 h postinjection. Notably, tumor fluorescence kept strong even after 48 h (Figure 2A), indicating that GE11-PS-DiR gives not only high accumulation but also good retention in SKOV3 ovarian tumor. In contrast, significantly less tumor accumulation was detected for the nontargeted PS-DiR control, confirming the active targeting effect of GE11-PS to SKOV3 ovarian tumor.

DOI: 10.1021/acs.molpharmaceut.8b00024
Mol. Pharmaceutics 2018, 15, 3664−3671

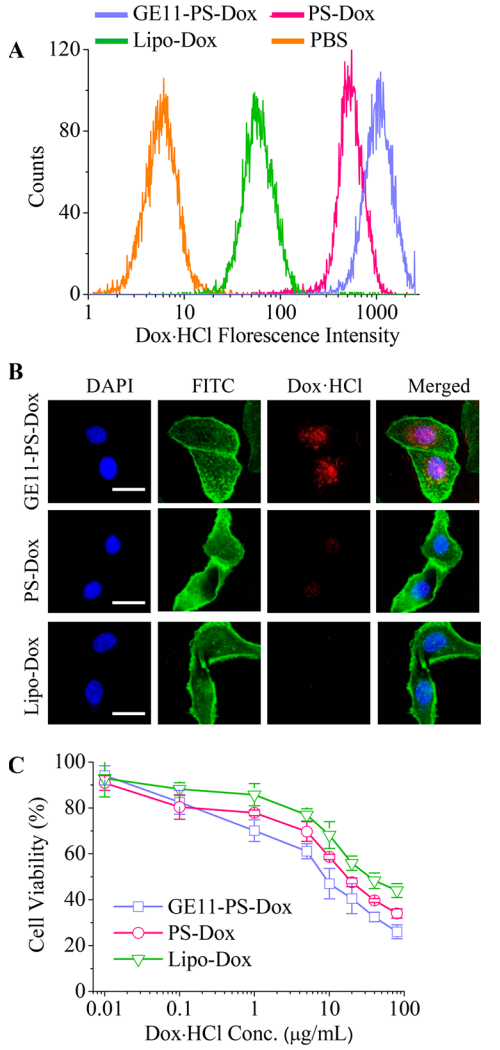

Figure 1. (A) Flow cytometric analyses of SKOV3 cells following 4 h incubation with GE11-PS-Dox, PS-Dox, Lipo-Dox, and PBS. The Dox·HCl dosage was 10.0 μg/mL. (B) CLSM images of SKOV3 cells after 4 h incubation with GE11-PS-Dox and another 8 h culture in fresh medium (Dox·HCl dosage: 10.0 μg/mL). For each panel, the images from left to right show cell nuclei stained by DAPI, cytoskeleton stained by phalloidin-FITC, Dox fluorescence, and overlays of the three images. Scale bars: 20 μm. (C) MTT assays of GE11-PS-Dox in SKOV3 cells. The cells were incubated with GE11-PS-Dox at varying concentrations of 0.01−40 μg of Dox·HCl equiv/mL for 4 h and further cultured in fresh medium for 44 h. The data are presented as mean ± SD (n = 4). PS-Dox and Lipo-Dox were used as controls.

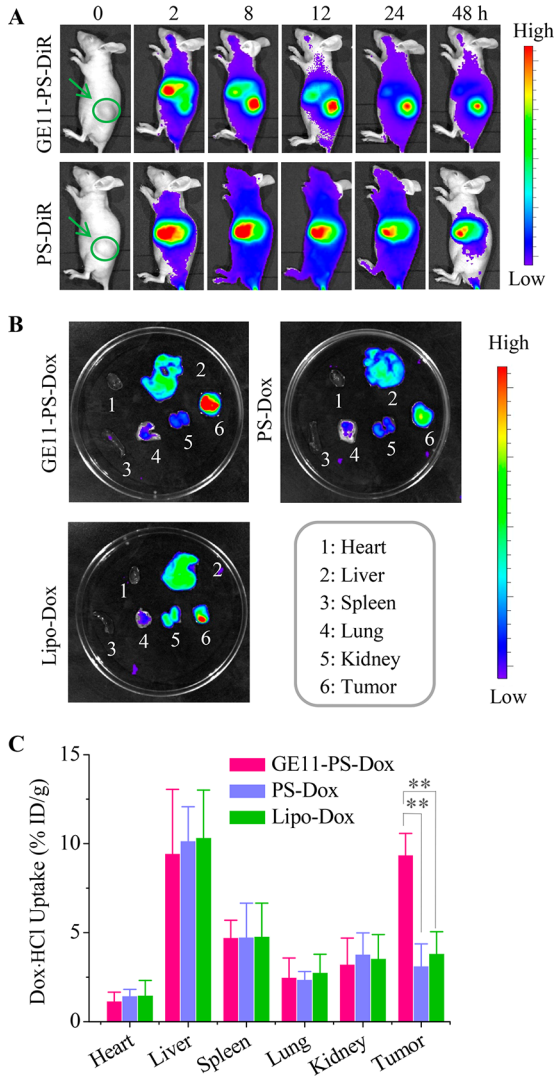

Figure 2. (A) *In vivo* NIR fluorescence images of SKOV3 tumor-bearing nude mice after *i.v.* administration of GE11-PS-DiR or PS-DiR (0.2 mg of DiR equiv/kg). (B) *Ex vivo* Dox fluorescence images of tumors and major organs 8 h postinjection of GE11-PS-Dox, PS-Dox, or Lipo-Dox (10 mg of Dox·HCl equiv/kg). (C) Quantification of Dox in tumors and major organs using fluorometry. Data are presented as mean ± SD (n = 3). One-way ANOVA and Tukey multiple comparisons tests, $^{**}p < 0.01$.

We further studied the *in vivo* biodistribution of GE11-PS-Dox in SKOV3 tumor-bearing mice. Interestingly, the mice treated with GE11-PS-Dox had the strongest Dox fluorescence in the tumor as seen from the *ex vivo* fluorescence imaging (Figure 2B), supporting high tumor accumulation and efficient drug release from GE11-PS-Dox. In contrast, Dox fluorescence in the tumor of the mice treated with PS-Dox and Lipo-Dox was comparably weak. Remarkably, quantification of Dox showed a high tumor accumulation of 9.37%ID/g for GE11-PS-Dox at 8 h postinjection, which was about 3.0- and 2.5-fold higher than that for PS-Dox and Lipo-Dox, respectively (Figure 2C), corroborating that GE11 peptide facilitates active targeting to EGFR overexpressing SKOV3 tumor.[51] GE11-PS-Dox not only exploits the enhanced permeability and retention (EPR) effect of tumor but also enhances its binding to and uptake by tumor cells, leading to further enhanced tumor accumulation and retention compared with the nontargeted controls that passively target to tumor. It should be noted that GE11-PS-Dox caused also high Dox accumulation in the liver, as typically observed for nanoformulations.[52,53] The Dox·HCl uptake in Figure 2C is the sum of released Dox·HCl and Dox·HCl encapsulated in liposome or polymersome formulations. As shown in Figure 2B, Dox fluorescence in the liver was significantly weaker than in the tumor, indicating a comparably lower free Dox concentration in the liver tissue. We and others have shown that Dox fluorescence is self-quenched when kept inside the nanoparticles due to homo-Förster resonance energy transfer (homo-FRET) effect.[47,54,55] All results point out that GE11-PS-Dox releases Dox·HCl more efficiently in the tumor site than in the liver tissue at 8 h postinjection. The corresponding tumor-to-normal tissue (T/N) distribution ratios of Dox further demonstrate 2.7−3.7-fold enhanced

DOI: 10.1021/acs.molpharmaceut.8b00024
Mol. Pharmaceutics 2018, 15, 3664−3671

selectivity of GE11-PS-Dox toward SKOV3 tumor as compared with Lipo-Dox and PS-Dox (Table S1). These results confirm that GE11-PS-Dox has superior targetability toward SKOV3 tumor to Lipo-Dox.

Targeted Treatment of SKOV3 Human Ovarian Tumor-Bearing Mice. We have shown previously that GE11-PS-Dox has an extraordinary maximum-tolerated dose (MTD) of >160 mg of Dox·HCl equiv/kg in mice, over 8-fold exceeding that of Lipo-Dox.[44] Herein, we were determined to examine the therapeutic efficacy of GE11-PS-Dox at a dosage of 12 mg of Dox·HCl equiv/kg in SKOV3 tumor-bearing mice because this treatment scheme has led to effective suppression of orthotopic SMMC-7721 tumor without causing obvious systemic toxicity. GE11-PS-Dox was intravenously given every 3 days and for a total of five injections. GE11-PS-Dox, PS-Dox, and Lipo-Dox at a dosage of 6 mg of Dox·HCl equiv/kg were used as controls. Figure 3A reveals that at the same dosage of 6 mg of Dox·HCl equiv/kg, nontargeted PS-Dox induced comparable tumor growth inhibition to Lipo-Dox but was apparently less effective than GE11-PS-Dox. Notably, GE11-PS-Dox at 12 mg of Dox·HCl equiv/kg caused significantly better tumor growth suppression than all three controls ($p < 0.01$). Moreover, in contrast to Lipo-Dox that caused significant body weight loss (up to 19%), no decrease of body weight was observed for GE11-PS-Dox (Figure 3B), supporting that GE11-PS-Dox induces far less adverse effects than Lipo-Dox. Remarkably, the survival rates demonstrated that all mice treated with GE11-PS-Dox at 12 mg/kg survived over the observation period of 78 days (Figure 3C). In contrast, control groups treated with Lipo-Dox, PS-Dox, and GE11-PS-Dox at 6 mg/kg all died in 55, 68, and 78 days, respectively. Notably, mice treated with GE11-PS-Dox at 6 mg/kg had significantly longer median survival time than those with Lipo-Dox and PS-Dox. Hematoxylin and eosin (H&E) staining displayed that GE11-PS-Dox caused significantly more severe necrosis of tumor tissue than Lipo-Dox (Figure S1). Moreover, as compared to Lipo-Dox, GE11-PS-Dox at either 6 or 12 mg of Dox·HCl equiv/kg induced obviously less harm to the major organs of mice including heart, liver, and kidney. The results at hand demonstrate that GE11-PS-Dox is a significantly more potent and less toxic alternative to Lipo-Dox for treatment of SKOV3 ovarian tumors *in vivo*.

Single Dose Treatment of SKOV3 Human Ovarian Tumor-Bearing Mice. To further investigate its therapeutic potential, a single dose of GE11-PS-Dox at 60 mg of Dox·HCl equiv/kg was attempted, given the fact that GE11-PS-Dox has a high MTD of over 160 mg of Dox·HCl equiv/kg. Lipo-Dox at a dosage of 15 mg of Dox·HCl equiv/kg was applied for comparison. No higher Lipo-Dox was tested because it has an MTD of less than 20 mg of Dox·HCl equiv/kg.[40,44] The results revealed that GE11-PS-Dox significantly suppressed tumor progression, while Lipo-Dox had little inhibitory effect (Figure 4A). The photograph of tumors of different groups on day 24 confirmed that a single dose of GE11-PS-Dox led to the smallest tumor size (Figure 4B). Little body weight change was observed for both GE11-PS-Dox and Lipo-Dox groups (Figure 4C), indicating that this treatment scheme can be well tolerated. In accordance, single dose treatment with GE11-PS-Dox resulted in significantly improved mice survival rate as compared to Lipo-Dox and PBS controls (median survival time: 66 versus 41 and 38 days, respectively) (Figure 4D). It should further be noted that given its high tolerated dose of over 160 mg of Dox·HCl equiv/kg, there remains a big window

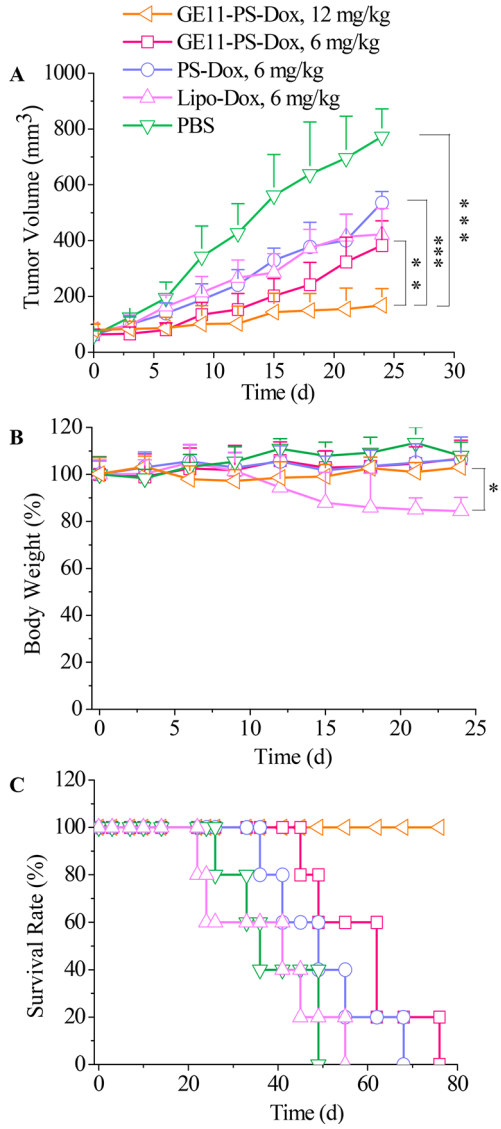

Figure 3. *In vivo* treatment of SKOV3 tumor-bearing nude mice with GE11-PS-Dox, which was given on day 0, 3, 6, 9, and 12 (dosage: 12 mg of Dox·HCl equiv/kg). GE11-PS-Dox, PS-Dox, and Lipo-Dox at 6 mg of Dox·HCl equiv/kg and PBS were used as controls. (A) Tumor volume of mice in 24 days; one-way ANOVA and Tukey multiple comparisons tests, $^{**}p < 0.01$, $^{***}p < 0.001$. (B) Body weight changes within 24 days; one-way ANOVA and Tukey multiple comparisons tests, $^{*}p < 0.05$; (C) Survival rates of mice within 78 days; Kaplan–Meier analysis with log-rank test for comparison: GE11-PS-Dox (6 mg/kg) vs Lipo-Dox and PS-Dox (6 mg/kg), $^{*}p < 0.05$. Data are presented as mean ± SD ($n = 5$).

to increase dosage of GE11-PS-Dox, which would likely further boost treatment effect toward SKOV3 human ovarian tumor-bearing mice. This single dose treatment scheme is advantageous over the traditional multiple dose scheme, as it would greatly reduce hospital cost, mitigate possible drug resistance, and increase patient quality of life.

CONCLUSION

We have shown that GE11-modified reversibly cross-linked polymersomal doxorubicin GE11-PS-Dox exhibits superior therapeutic efficacy and safety profile to clinically used Lipo-Dox in EGFR overexpressing SKOV3 ovarian tumor xenografts in nude mice. Our results disclose that GE11-PS-Dox can

DOI: 10.1021/acs.molpharmaceut.8b00024
Mol. Pharmaceutics 2018, 15, 3664−3671

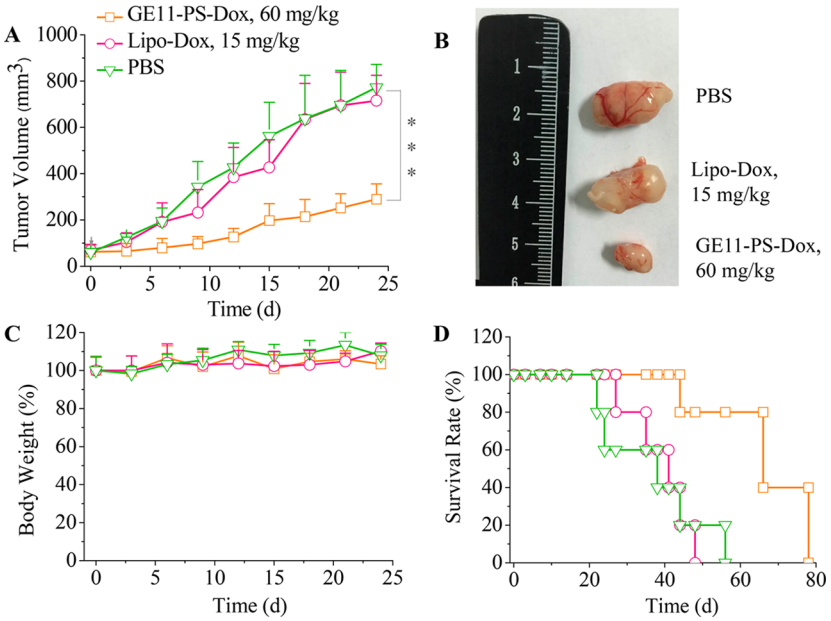

Figure 4. Single dose treatment of SKOV3 tumor-bearing nude mice with GE11-PS-Dox at 60 mg of Dox·HCl equiv/kg. PBS and a single dose of Lipo-Dox at 15 mg of Dox·HCl equiv/kg were used as controls. (A) Tumor volume of mice in 24 days (n = 5); one-way ANOVA and Tukey multiple comparisons tests, ***p < 0.001. (B) Photograph of tumors of different groups on day 24. (C) Body weight changes of mice within 24 days. (D) Survival rates of mice within 78 days. Data are presented as mean ± SD. Kaplan−Meier analysis with log-rank test for comparison: GE11-PS-Dox vs Lipo-Dox or PBS, **p < 0.01.

actively target and release Dox to SKOV3 cells *in vitro* and *in vivo*. It is remarkable that mice treated with five doses of GE11-PS-Dox (12 mg of Dox equiv/kg) all have survived over an experimental period of 78 days. More interestingly, a single dose of GE11-PS-Dox at 60 mg of Dox equiv/kg can also significantly inhibit tumor progression and prolong survival rate, without inducing obvious side effects. GE11-PS-Dox, given either in multiple or single dosage scheme, outperforms Lipo-Dox in treating SKOV3 tumor-bearing mice. This GE11 peptide-functionalized reversibly cross-linked polymersomal doxorubicin has emerged as an advanced alternative to Lipo-Dox for safer and targeted treatment of EGFR overexpressing SKOV3 human ovarian tumor.

■ ASSOCIATED CONTENT

Supporting Information

The Supporting Information is available free of charge on the ACS Publications website at DOI: 10.1021/acs.molpharmaceut.8b00024.

Details of materials, characterization, and methods of MTT assays (PDF)

■ AUTHOR INFORMATION

Corresponding Authors

*Tel/Fax: +86-512-65880098. E-mail: fhmeng@suda.edu.cn.
*E-mail: zyzhong@suda.edu.cn.

ORCID

Fenghua Meng: 0000-0002-8608-7738
Zhiyuan Zhong: 0000-0003-4175-4741

Notes

The authors declare no competing financial interest.

■ ACKNOWLEDGMENTS

This work is supported by the National Natural Science Foundation of China (51473111, 51633005, 51773146, and 51561135010).

■ REFERENCES

(1) Patch, A.-M.; Christie, E. L.; Etemadmoghadam, D.; Garsed, D. W.; George, J.; Fereday, S.; Nones, K.; Cowin, P.; Alsop, K.; Bailey, P. J. Whole−Genome Characterization of Chemoresistant Ovarian Cancer. *Nature* **2015**, *521*, 489−494.

(2) Kipps, E.; Tan, D. S.; Kaye, S. B. Meeting the Challenge of Ascites in Ovarian Cancer: New Avenues for Therapy and Research. *Nat. Rev. Cancer* **2013**, *13*, 273−282.

(3) Jayson, G. C.; Kohn, E. C.; Kitchener, H. C.; Ledermann, J. A. Ovarian Cancer. *Lancet* **2014**, *384*, 1376−1388.

(4) Banerjee, S.; Kaye, S. B. New Strategies in the Treatment of Ovarian Cancer: Current Clinical Perspectives and Future Potential. *Clin. Cancer Res.* **2013**, *19*, 961−968.

(5) Coleman, R. L.; Monk, B. J.; Sood, A. K.; Herzog, T. J. Latest Research and Treatment of Advanced-Stage Epithelial Ovarian Cancer. *Nat. Rev. Clin. Oncol.* **2013**, *10*, 211−224.

(6) Pham, E.; Birrer, M. J.; Eliasof, S.; Garmey, E. G.; Lazarus, D.; Lee, C. R.; Man, S.; Matulonis, U. A.; Peters, C. G.; Xu, P.; Krasner, C.; Kerbel, R. S. Translational Impact of Nanoparticle−Drug Conjugate CRLX101 with or without Bevacizumab in Advanced Ovarian Cancer. *Clin. Cancer Res.* **2015**, *21*, 808−818.

(7) He, C.; Poon, C.; Chan, C.; Yamada, S. D.; Lin, W. Nanoscale Coordination Polymers Codeliver Chemotherapeutics and siRNAs to Eradicate Tumors of Cisplatin-Resistant Ovarian Cancer. *J. Am. Chem. Soc.* **2016**, *138*, 6010−6019.

(8) Lin, C.-J.; Kuan, C.-H.; Wang, L.-W.; Wu, H.-C.; Chen, Y.; Chang, C.-W.; Huang, R.-Y.; Wang, T.-W. Integrated Self-Assembling Drug Delivery System Possessing Dual Responsive and Active Targeting for Orthotopic Ovarian Cancer Theranostics. *Biomaterials* **2016**, *90*, 12−26.

(9) Sapiezynski, J.; Taratula, O.; Rodriguez-Rodriguez, L.; Minko, T. Precision Targeted Therapy of Ovarian Cancer. *J. Controlled Release* **2016**, *243*, 250−268.

DOI: 10.1021/acs.molpharmaceut.8b00024
Mol. Pharmaceutics 2018, 15, 3664−3671

(10) Hadla, M.; Palazzolo, S.; Corona, G.; Caligiuri, I.; Canzonieri, V.; Toffoli, G.; Rizzolio, F. Exosomes Increase the Therapeutic Index of Doxorubicin in Breast and Ovarian Cancer Mouse Models. *Nanomedicine* **2016**, *11*, 2431−2441.
(11) Zahedi, P.; De Souza, R.; Huynh, L.; Piquette-Miller, M.; Allen, C. Combination Drug Delivery Strategy for the Treatment of Multidrug Resistant Ovarian Cancer. *Mol. Pharmaceutics* **2011**, *8*, 260−269.
(12) Allen, T. M.; Cullis, P. R. Liposomal Drug Delivery Systems: From Concept to Clinical Applications. *Adv. Drug Delivery Rev.* **2013**, *65*, 36−48.
(13) Barenholz, Y. C. Doxil®—the First FDA-Approved Nano-Drug: Lessons Learned. *J. Controlled Release* **2012**, *160*, 117−134.
(14) Blanco, E.; Shen, H.; Ferrari, M. Principles of Nanoparticle Design for Overcoming Biological Barriers to Drug Delivery. *Nat. Biotechnol.* **2015**, *33*, 941−951.
(15) Seynhaeve, A. L.; Dicheva, B. M.; Hoving, S.; Koning, G. A.; ten Hagen, T. L. Intact Doxil Is Taken up Intracellularly and Released Doxorubicin Sequesters in the Lysosome: Evaluated by in Vitro/in Vivo Live Cell Imaging. *J. Controlled Release* **2013**, *172*, 330−340.
(16) Slingerland, M.; Guchelaar, H.-J.; Gelderblom, H. Liposomal Drug Formulations in Cancer Therapy: 15 Years Along the Road. *Drug Discovery Today* **2012**, *17*, 160−166.
(17) Noble, G. T.; Stefanick, J. F.; Ashley, J. D.; Kiziltepe, T.; Bilgicer, B. Ligand-Targeted Liposome Design: Challenges and Fundamental Considerations. *Trends Biotechnol.* **2014**, *32*, 32−45.
(18) Shah, V.; Taratula, O.; Garbuzenko, O. B.; Taratula, O. R.; Rodriguez-Rodriguez, L.; Minko, T. Targeted Nanomedicine for Suppression of CD44 and Simultaneous Cell Death Induction in Ovarian Cancer: An Optimal Delivery of siRNA and Anticancer Drug. *Clin. Cancer Res.* **2013**, *19*, 6193−6204.
(19) Pattni, B. S.; Chupin, V. V.; Torchilin, V. P. New Developments in Liposomal Drug Delivery. *Chem. Rev.* **2015**, *115*, 10938−10966.
(20) Ying, M.; Shen, Q.; Yu, L.; Yan, Z.; Wei, X.; Zhan, C.; Jie, G.; Cao, X.; Yao, B.; Lu, W. Stabilized Heptapeptide A7R for Enhanced Multifunctional Liposome-Based Tumor-Targeted Drug Delivery. *ACS Appl. Mater. Interfaces* **2016**, *8*, 13232−13241.
(21) Min, H. K.; Yoo, H. J.; Kwon, Y. H.; Yoon, H. Y.; Sang, G. L.; Kim, S. R.; Dong, W. Y.; Kang, M. J.; Choi, Y. W. Design of Multifunctional Liposomal Nanocarriers for Folate Receptor-Specific Intracellular Drug Delivery. *Mol. Pharmaceutics* **2015**, *12*, 4200−4213.
(22) Wang, Y.; Zhou, J.; Qiu, L.; Wang, X.; Chen, L.; Liu, T.; Di, W. Cisplatin−Alginate Conjugate Liposomes for Targeted Delivery to EGFR-Positive Ovarian Cancer Cells. *Biomaterials* **2014**, *35*, 4297−4309.
(23) Brinkman, A. M.; Chen, G.; Wang, Y.; Hedman, C. J.; Sherer, N. M.; Havighurst, T. C.; Gong, S.; Xu, W. Aminoflavone-Loaded EGFR-Targeted Unimolecular Micelle Nanoparticles Exhibit Anti-Cancer Effects in Triple Negative Breast Cancer. *Biomaterials* **2016**, *101*, 20−31.
(24) Mickler, F. M.; Möckl, L.; Ruthardt, N.; Ogris, M.; Wagner, E.; Bräuchle, C. Tuning Nanoparticle Uptake: Live-Cell Imaging Reveals Two Distinct Endocytosis Mechanisms Mediated by Natural and Artificial EGFR Targeting Ligand. *Nano Lett.* **2012**, *12*, 3417−3423.
(25) Talekar, M.; Ganta, S.; Singh, A.; Amiji, M.; Kendall, J.; Denny, W. A.; Garg, S. Phosphatidylinositol 3-Kinase Inhibitor (PIK75) Containing Surface Functionalized Nanoemulsion for Enhanced Drug Delivery, Cytotoxicity and Pro-Apoptotic Activity in Ovarian Cancer Cells. *Pharm. Res.* **2012**, *29*, 2874−2886.
(26) Genta, I.; Chiesa, E.; Colzani, B.; Modena, T.; Conti, B.; Dorati, R. GE11 Peptide as an Active Targeting Agent in Antitumor Therapy: A Minireview. *Pharmaceutics* **2018**, *10*, 2−16.
(27) Tang, H.; Chen, X.; Rui, M.; Sun, W.; Chen, J.; Peng, J.; Xu, Y. Effects of Surface Displayed Targeting Ligand GE11 on Liposome Distribution and Extravasation in Tumor. *Mol. Pharmaceutics* **2014**, *11*, 3242−3250.
(28) Lee, J. S.; Feijen, J. Polymersomes for Drug Delivery: Design, Formation and Characterization. *J. Controlled Release* **2012**, *161*, 473−483.
(29) Balasubramanian, V.; Herranz-Blanco, B.; Almeida, P. V.; Hirvonen, J.; Santos, H. A. Multifaceted Polymersome Platforms: Spanning from Self-Assembly to Drug Delivery and Protocells. *Prog. Polym. Sci.* **2016**, *60*, 51−85.
(30) Kim, S.-H.; Kim, J. W.; Kim, D.-H.; Han, S.-H.; Weitz, D. A. Polymersomes Containing a Hydrogel Network for High Stability and Controlled Release. *Small* **2013**, *9*, 124−131.
(31) Song, Z.; Huang, Y.; Prasad, V.; Baumgartner, R.; Zhang, S.; Harris, K.; Katz, J. S.; Cheng, J. Preparation of Surfactant-Resistant Polymersomes with Ultrathick Membranes through RAFT Dispersion Polymerization. *ACS Appl. Mater. Interfaces* **2016**, *8*, 17033−17037.
(32) Wang, X.; Hu, J.; Liu, G.; Tian, J.; Wang, H.; Gong, M.; Liu, S. Reversibly Switching Bilayer Permeability and Release Modules of Photochromic Polymersomes Stabilized by Cooperative Noncovalent Interactions. *J. Am. Chem. Soc.* **2015**, *137*, 15262−15275.
(33) Hu, X.; Zhang, Y.; Xie, Z.; Jing, X.; Bellotti, A.; Gu, Z. Stimuli-Responsive Polymersomes for Biomedical Applications. *Biomacromolecules* **2017**, *18*, 649−673.
(34) Kim, H.; Kang, Y. J.; Kang, S.; Kim, K. T. Monosaccharide-Responsive Release of Insulin from Polymersomes of Polyboroxole Block Copolymers at Neutral pH. *J. Am. Chem. Soc.* **2012**, *134*, 4030−4033.
(35) Liu, G.; Wang, X.; Hu, J.; Zhang, G.; Liu, S. Self-Immolative Polymersomes for High-Efficiency Triggered Release and Programmed Enzymatic Reactions. *J. Am. Chem. Soc.* **2014**, *136*, 7492−7497.
(36) Che, H.; van Hest, J. C. Stimuli-Responsive Polymersomes and Nanoreactors. *J. Mater. Chem. B* **2016**, *4*, 4632−4647.
(37) Zhu, D.; Wu, S.; Hu, C.; Chen, Z.; Wang, H.; Fan, F.; Qin, Y.; Wang, C.; Sun, H.; Leng, X.; Kong, D.; Zhang, L. Folate-Targeted Polymersomes Loaded with Both Paclitaxel and Doxorubicin for the Combination Chemotherapy of Hepatocellular Carcinoma. *Acta Biomater.* **2017**, *58*, 399−412.
(38) Egli, S.; Nussbaumer, M. G.; Balasubramanian, V.; Chami, M.; Bruns, N.; Palivan, C.; Meier, W. Biocompatible Functionalization of Polymersome Surfaces: A New Approach to Surface Immobilization and Cell Targeting Using Polymersomes. *J. Am. Chem. Soc.* **2011**, *133*, 4476−4483.
(39) Yassin, M. A.; Appelhans, D.; Wiedemuth, R.; Formanek, P.; Boye, S.; Lederer, A.; Temme, A.; Voit, B. Overcoming Concealment Effects of Targeting Moieties in the PEG Corona: Controlled Permeable Polymersomes Decorated with Folate-Antennae for Selective Targeting of Tumor Cells. *Small* **2015**, *11*, 1580−1591.
(40) Zhang, N.; Xia, Y.; Zou, Y.; Yang, W.; Zhang, J.; Zhong, Z.; Meng, F. ATN-161 Peptide Functionalized Reversibly Cross-Linked Polymersomes Mediate Targeted Doxorubicin Delivery into Melanoma-Bearing C57BL/6 Mice. *Mol. Pharmaceutics* **2016**, *14*, 2538−2547.
(41) Yang, W.; Xia, Y.; Zou, Y.; Meng, F.; Zhang, J.; Zhong, Z. Bioresponsive Chimaeric Nano-Polymersomes Enable Targeted and Efficacious Protein Therapy for Human Lung Cancers in Vivo. *Chem. Mater.* **2017**, *29*, 8757−8765.
(42) Yang, W.; Zou, Y.; Meng, F.; Zhang, J.; Cheng, R.; Deng, C.; Zhong, Z. Efficient and Targeted Suppression of Human Lung Tumor Xenografts in Mice with Methotrexate Sodium Encapsulated in All-Function-in-One Chimeric Polymersomes. *Adv. Mater.* **2016**, *28*, 8234−8239.
(43) Zou, Y.; Meng, F.; Deng, C.; Zhong, Z. Robust, Tumor-Homing and Redox-Sensitive Polymersomal Doxorubicin: A Superior Alternative to Doxil and Caelyx? *J. Controlled Release* **2016**, *239*, 149−158.
(44) Fang, Y.; Yang, W.; Cheng, L.; Meng, F.; Zhang, J.; Zhong, Z. EGFR-Targeted Multifunctional Polymersomal Doxorubicin Induces Selective and Potent Suppression of Orthotopic Human Liver Cancer in Vivo. *Acta Biomater.* **2017**, *64*, 323−333.
(45) Shir, A.; Ogris, M.; Roedl, W.; Wagner, E.; Levitzki, A. EGFR-Homing dsRNA Activates Cancer-Targeted Immune Response and Eliminates Disseminated EGFR-Overexpressing Tumors in Mice. *Clin. Cancer Res.* **2011**, *17*, 1033−1043.
(46) Chen, J.; Ouyang, J.; Chen, Q.; Deng, C.; Meng, F.; Zhang, J.; Cheng, R.; Lan, Q.; Zhong, Z. EGFR and CD44 Dual-Targeted

DOI: 10.1021/acs.molpharmaceut.8b00024
Mol. Pharmaceutics 2018, 15, 3664−3671

Multifunctional Hyaluronic Acid Nanogels Boost Protein Delivery to Ovarian and Breast Cancers in Vitro and in Vivo. *ACS Appl. Mater. Interfaces* **2017**, *9*, 24140−24147.
(47) Zhu, Y.; Zhang, J.; Meng, F.; Deng, C.; Cheng, R.; Feijen, J.; Zhong, Z. cRGD-Functionalized Reduction-Sensitive Shell-Sheddable Biodegradable Micelles Mediate Enhanced Doxorubicin Delivery to Human Glioma Xenografts in Vivo. *J. Controlled Release* **2016**, *233*, 29−38.
(48) Pujade-Lauraine, E.; Wagner, U.; Aavall-Lundqvist, E.; Gebski, V.; Heywood, M.; Vasey, P. A.; Volgger, B.; Vergote, I.; Pignata, S.; Ferrero, A.; Sehouli, J.; Lortholary, A.; Kristensen, G.; Jackisch, C.; Joly, F.; Brown, C.; Le Fur, N.; du Bois, A. Pegylated Liposomal Doxorubicin and Carboplatin Compared with Paclitaxel and Carboplatin for Patients with Platinum-Sensitive Ovarian Cancer in Late Relapse. *J. Clin. Oncol.* **2010**, *28*, 3323−3329.
(49) Lombardi, G.; Zustovich, F.; Farinati, F.; Cillo, U.; Vitale, A.; Zanus, G.; Donach, M.; Farina, M.; Zovato, S.; Pastorelli, D. Pegylated Liposomal Doxorubicin and Gemcitabine in Patients with Advanced Hepatocellular Carcinoma. *Cancer* **2011**, *117*, 125−133.
(50) Mahner, S.; Meier, W.; du Bois, A.; Brown, C.; Lorusso, D.; Dell'Anna, T.; Cretin, J.; Havsteen, H.; Bessette, P.; Zeimet, A. G.; Vergote, I.; Vasey, P.; Pujade-Lauraine, E.; Gladieff, L.; Ferrero, A. Carboplatin and Pegylated Liposomal Doxorubicin Versus Carboplatin and Paclitaxel in Very Platinum-Sensitive Ovarian Cancer Patients: Results from a Subset Analysis of the Calypso Phase III Trial. *Eur. J. Cancer* **2015**, *51*, 352−358.
(51) Milane, L.; Duan, Z.; Amiji, M. Development of EGFR-Targeted Polymer Blend Nanocarriers for Combination Paclitaxel/Lonidamine Delivery to Treat Multi-Drug Resistance in Human Breast and Ovarian Tumor Cells. *Mol. Pharmaceutics* **2010**, *8*, 185−203.
(52) Blanco, E.; Shen, H.; Ferrari, M. Principles of Nanoparticle Design for Overcoming Biological Barriers to Drug Delivery. *Nat. Biotechnol.* **2015**, *33*, 941−951.
(53) Maeda, H.; Nakamura, H.; Fang, J. The EPR Effect for Macromolecular Drug Delivery to Solid Tumors: Improvement of Tumor Uptake, Lowering of Systemic Toxicity, and Distinct Tumor Imaging in Vivo. *Adv. Drug Delivery Rev.* **2013**, *65*, 71−79.
(54) Rowland, C. E.; Delehanty, J. B.; Dwyer, C. L.; Medintz, I. L. Growing Applications for Bioassembled Förster Resonance Energy Transfer Cascades. *Mater. Today* **2017**, *20*, 131−141.
(55) Nicoli, F.; Barth, A.; Bae, W.; Neukirchinger, F.; Crevenna, A. H.; Lamb, D. C.; Liedl, T. Directional Photonic Wire Mediated by Homo-Förster Resonance Energy Transfer on a DNA Origami Platform. *ACS Nano* **2017**, *11*, 11264−11272.

DOI: 10.1021/acs.molpharmaceut.8b00024
Mol. Pharmaceutics 2018, 15, 3664−3671